In-Line Characterization of Polypropylene Nanocomposites Using FT-NIR

Andreas Witschnigg,[1] Stephan Laske,[1] Milan Kracalik,[1] Michael Feuchter,[2] Gerald Pinter,[2] Günther Maier,[3] Wolfgang Märzinger,[4] Michael Haberkorn,[5] Günter Rüdiger Langecker,[1] Clemens Holzer[1]

[1]*Institute of Plastics Processing, University of Leoben, Leoben 8700, Austria*
[2]*Institute of Materials Science and Testing of Plastics, University of Leoben, Leoben 8700, Austria*
[3]*Material Center Leoben, Leoben 8700, Austria*
[4]*i-RED Infrarot Systeme GmbH, Hafenstrasse 47-51, Linz 4020, Austria*
[5]*RECENDT GmbH, Hafenstrasse 47-51, Linz 4020, Austria*

Received 22 October 2009; accepted 27 December 2009
DOI 10.1002/app.32024
Published online 29 April 2010 in Wiley InterScience (www.interscience.wiley.com).

ABSTRACT: The morphology of polymer nanocomposites is usually characterized by various methods like X-ray diffraction (XRD) or transmission electron microscopy (TEM). In this work, a new approach for characterizing nanocomposites is developed: the results of small angle x-ray scattering, on-line extensional rheometry (level of melt strength) and Young's modulus out of tensile test are correlated with those of near infrared (NIR) spectroscopy. The disadvantages of the common characterization methods are high costs and very time consuming sample preparation and testing. In contrast, NIR spectroscopy has the advantage to be measured in-line and in real time directly in the melt. The results were obtained for different aggregate states (NIR spectroscopy and on-line rheotens test in melt state, tensile test, and XRD in solid state). Therefore, important factors like crystallization could not be considered. Nevertheless, this work demonstrates that the NIR-technology is perfectly suitable for quantitative in-line characterization. The results show that, by the installation of a NIR spectrometer on a nanocomposite-processing compounder, a powerful instrument for quality control and optimization of compounding process, in terms of increased and constant quality, is available. © 2010 Wiley Periodicals, Inc. J Appl Polym Sci 117: 3047–3053, 2010

Key words: nanoparticles; polymer composite materials; FTNIR spectroscopy

INTRODUCTION

The use of nanocomposites has developed rapidly over the last years. One reason is their great potential for improving material properties with only a small amount of filler. Nanocomposites are polymers filled with particles where at least one dimension is in the order of nanometers. There are several types of nanofillers, which are classified in three structures (spherical, laminar, or fibrous particles). Because of the high aspect ratio, which is linked with the ability to improve polymers, fibrous, and laminar particles are commonly used.

There are two reasons for the improvement of material properties by the application of nanofillers. The first reason is the enforcement of the polymer matrix by means of the particles (like it is the case for other fillers). The second effect is the movement-restrictive effect on the polymer chains caused by the layered anorganic nanofillers. Therefore mainly layered silicates (most common montmorillonite) with an aspect ratio up to 1000 are used.

To reach best interactions between polymer matrix and nanofiller (especially layered silicates) a homogeneous dispersion is essential. Because of the technological simplicity, nanocomposites are preferably produced by using a twin screw extruder operating at high temperatures and pressures.[1,2] Shearing forces, induced by the rotation of the screw and thermodynamical interactions between polymer chain and layered silicate clay are delaminating the layered silicate. During the process, the structures which are responsible for the level of reinforcement are formed by physical bonding between the hydrophilic clay, the hydrophobic polymer matrix and a compatibilizer.[3]

According to the dispersion and the homogeneity of the nanofiller conventional composites, intercalated nanocomposites and exfoliated nanocomposites can be formed. To determine the homogeneity of the material a variety of methods are commonly used. These include optical [scanning (SEM) and transmission (TEM) electron microscopy], mechanical (tensile

Correspondence to: S. Laske (stephan.laske@unileoben.ac.at).

Contract grant sponsor: Austrian Nano Initiative (project Nanocomp – 0901 PlaComp1).

strength, extensional rheology) and light scattering methods (small angle (SAXS) and wide angle (WAXS) X-ray scattering). A new way to determine material homogeneity is the use of near infrared (NIR) spectroscopy. NIR spectroscopy is a nondestructive, optical method to obtain information about the composition of samples and interactions within the sample. Near- and mid-infrared methods (NIR, MIR) measure the absorbance of light due to excitation of molecular vibrations of the substance under investigation. Mid-infrared measurements (often referred to only as IR) are exploiting radiation in a spectral range between 2500 and 25,000 nm, detecting fundamental molecular vibrations, while NIR is operating in the spectral range between 780 and 2500 nm. Therefore NIR detects the overtones and combinations of the molecular vibrations. Although NIR signals are 100–1000 times weaker than IR signals, only the NIR technique is suitable for in-line implementation due to the use of quartz based optics and optical fibers for signal transfer from the measuring probe to the NIR spectrometer.

If light is transmitted through a sample, vibrations of the molecular bondings are excited, resulting in an energy absorbance at specific wavelengths depending on the type of molecule and molecular bondings, which can be detected by NIR spectroscopy. The wavelength position of the absorbance bands in the NIR spectrum provides the information for identification of substances and chemical functionalities. The prevailing conditions in the sample (chemical state, number, and type of interactions) are narrowly linked with the mechanical properties, which can therefore be determined by NIR spectroscopy.[4]

NIR measurements have a variety of successful applications in polymer science, such as the analysis of polymerization or copolymerization (mostly done by detecting the characteristically absorption caused by chemical groups as e.g., OH groups or vinyl acetate groups in ethylene vinyl acetate), crystallinity, molecular weight, anisotropy, intermolecular interactions, molar mass, porosity, specific surface area, tacticity, orientation, concentrations of flame retardants (e.g., melamine cyanurate), density measurements, and other chemical processes that appear during polymer processing.[5–16]

In other studies, nanocomposites[6,15–17] are analyzed regarding crystallization properties and particle size[16] using NIR measurements.

The near infrared technique combined with stress–strain curves to evaluate filled rubbers (using SiO_2, TiO_2, layered silicate, and Nanotubes) with regard to changes in crystallization and degree of exfoliation under strain has also been investigated. A coherence between crystallization under strain and a shift in NIR spectra has been found.[17]

In addition, NIR spectroscopy has successfully been used to monitor the processing of pharmaceutical nanoparticles and to classify them by their particle size in a high solids dispersion.[18]

The analysis of the melt strength of a polypropylene (PP) nanocomposite with off-line NIR spectroscopy (correlated with off-line rheotens measurement) has already been achieved.[4]

EXPERIMENTAL

Materials

The isotactic PP homopolymer HC600TF (melt flow index (MFI) 2.8 g/10 min; 230°C/2.16 kg) was supplied by Borealis, Linz, Austria. The used nanofiller (montmorillonite intercalated with dimethyl distearyl ammonium chloride) with commercial indication Nanofil 5 was supplied by Sud-Chemie, Munich, Germany. The compatibilizer (Scona TPPP 2112 FA, MFI 14.8 g/10 min) was supplied by Kometra, Schkopau, Germany.

Preparation of polypropylene nanocomposites

For the compounding process, an intermeshing, corotating twin screw extruder Theysohn TSK30/40D (Theysohn Holding, Vienna, Austria) with a string die was used. The feed rate was set at 10 kg/h, with a screw speed from 100 to 300 rpm. The formulation of the nanocomposite was constant at 5 wt % organoclay, 5 wt % compatibilizer and 90 wt % polypropylene. A melt pump was used ($\Delta p \sim -100$ bar) to increase the residence time and shear rate and therefore improve the dispersion of the nanofiller. A bypass system was used to create a melt string for on-line rheotens measurement. Two different screw geometries, in the following referred to as geometry 1 and geometry 2, were used to produce nanocomposites with varying layer distance and mechanical properties. The main difference between these screw geometries is the number and position of kneading elements resulting in different values of induced shear energy and residence time. As can be seen in Figure 1, both geometries are identical until the side feeder. From this point, geometry 1 consists of a kneading block right after the side feeder followed by a short kneading block at the end of the screw for additional induced shear energy in the backpressure zone caused by the melt pump. In opposite to that, geometry 2 consists only of conveying blocks.

For structural and mechanical characterization, plates with a thickness of 2 mm and standard dog bone shaped specimens (150 mm length, 20 mm width, 4 mm thickness), respectively, were prepared using the hydraulic vacuum press machine (Collin

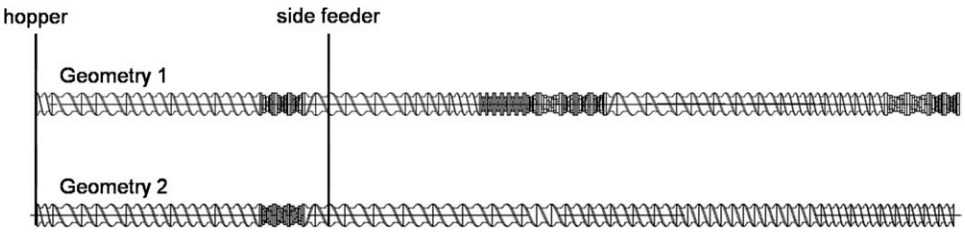

Figure 1 Schematically illustration of screw geometry 1 and 2.

200 PV, Dr. Collin, Ebersberg, Germany) and the injection molding machine (Engel ES330/80H, 800 KN closing force, Schwertberg, Austria).

Small angle x-ray scattering

X-ray measurements were performed using Bruker NanoSTAR (Bruker AXS, Karlsruhe, Germany) small angle X-ray scattering (SAXS) equipment. This system was equipped with a two dimensional X-ray detector. A wavelength of 0.154 nm (Cu-Kα) was used. The samples were measured in transmission at a temperature of 23°C. To avoid the influence of texture, all scattering measurements were performed on plate samples. The gallery period 1 of the nanofiller was determined on a powder sample. To avoid statistical effects, the scattering curves recorded at three different positions on the samples were averaged. To determine the gallery period, scattering curves were corrected for background scatter and a Lorenz correction was applied. The Lorenz correction was performed by multiplying the scattered intensity (I(q)) by q^2, q being the magnitude of the scattering vector. For the determination of the peak position the data were fitted with a Pseudo-Voigt function.[19] The interlayer distance is then calculated with the Bragg's law. The modulus of scattering vector q is defined as $q = (4\pi \sin\theta)/\lambda$ where λ is the wavelength of the used radiation and θ is the half of the scattering angle 2θ. The SAXS data evaluation was basically performed by applying a correlation function method according to Strobl and Schneider.[20]

Mechanical properties - tensile test

A universal tensile testing machine (Type: Z010, Zwick and Co. KG, Ulm, Germany) was used to carry out the tensile tests according to ISO 527–1. All tests were carried out under standardized conditions (23 ± 2°C/50 ± 5% r.H.). The data was evaluated using the testXpert II software (ZWICK, Ulm, Germany).

Rheotens measurements

The different physical crosslinking and bonding between polymer chains and organoclay results in a diversity of viscoelastic response. Therefore rheotens measurements are used to identify changes of the elongational viscosity. Individual nanoparticles act as entanglement or crosslinking sites and raise the extensional stiffness of the composite.[21]

The Rheotens 71.97 equipment (Göttfert, Buchen, Germany) was used. The melt string was applied through a bypass system directly from the extruder to achieve on-line measurement. Two or four rotating wheels (linearly accelerated) are connected to a force transducer while drawing off the extruded string until it breaks. The drawing force applied to the wheels at a specific draw rate is the reference value for the melt strength level. To compare the draw force level of different nanocomposite systems, the drawing force at a draw rate of 150 mm/s has been chosen as a comparative value. The data of at least three measurements for each sample were evaluated.

In-line FTNIR measurements

For in-line measurement a Fourier transform near infrared (FTNIR) spectrometer of i-Red Infrared Systems (Linz, Austria) with a probe installed right before the die was used. The spectrometer is working at a spectral range of 12,000 – 3800 cm^{-1} (900–2600 nm) with a spectral resolution of 1.5 cm^{-1}. The probe was connected to the spectrometer using fiber optics. The spectral data was collected with near infrared process spectrometer software (NIPS). The chemometric evaluation of the measured spectra was done with the software package Thermo GRAMS/AI from Thermo Fisher Scientific.

For a single spectrum 50 scans (10 scans per second) were averaged. For each setting 100 spectra were used to create a chemometrical model. To avoid drift effects caused by environmental or other parasitic effects, the measurement settings were chosen randomly.

Evaluation of NIR data

For the realization of an adequate process monitoring it is essential to find relations between composition of the sample, particle size or mechanical properties. This procedure is extensive, because NIR

measurements detect combinations of vibrations and overlapping bands. Therefore statistics provides various algorithms that establish a relationship between spectral data and a chemometric model. The intricacy for building a chemometric model is the problem of finding the right algorithm, the right preprocessing method and the right wavelength range. NIR measurements are in need of reference investigations (for linking them with mechanical properties), which are providing the values used for correlation with the spectral data. It is of immense importance for the accurateness of the chemometric model that these values are as precise as possible.

The multivariate data applied by NIR spectra are more dimensional (n-dimensional space). Therefore it is necessary to project the data on a two dimensional plane. The emerging picture is changing if the data points are rotated in the n-dimensional space. The possibilities of such projections are infinitive so it is essential to find the direction where the scatter along the axis reaches its maximum (maximum of information). If such a direction is found an axis orthogonal on the first axis is rotated until the scattering of data is reaching the maximum again. This approach is continued as all n-dimensions are considered. This procedure is defined mathematically as eigenvalue problem.

All performable evaluation methods, such as principal component analysis (PCA), principal component regression (PCR) or partial least squares (PLS 1 and PLS 2) are working basically on this approach.

It is of great advantage to exclude some regions with irrelevant spectral information. This can be done by calculating an absorption spectra out of two different spectra. This absorption spectra shows those wavelength regions with the highest difference and preferably low signal noise. This region can then be chosen to achieve good correlating chemometrical models.

Before the spectra are used for further calculation a preprocessing is often beneficial to get rid of parasitic effects like light straying caused by irregularities in the melt. One of the methods used is mean centering, which is calculating an average spectrum out of all used spectra and subtracts it from every single spectrum to get rid of offset effects. A way to achieve path length correction is to normalize the spectra to correct simple nonlinearities or to use algorithms such as standard normal variate transformation (SNV) or multiplicative scatter correction (MSC).

Experimentally NIR spectra of samples with varying but known responses were measured, pretreated and then the PLS 1 algorithm was used to generate a linear calibration model for calculating the responses from the measured NIR data using reference values. Then a cross validation was performed on the calculated chemometrical model. The principle of a cross validation is always the same. The model data are separated in two excluding sets (one experimental adjustment is sequentially left out). The bigger set is called training set and is used to calculate the model. The second set (test-set) is used to affirm the model. This procedure is repeated for all experimental adjustments. The bigger the training set gets the better cross validation works, especially when extrapolation is needed. The quality and the predictive ability of the model is rated basically with the coefficient of determination R^2 and the root mean square error of cross validation RMSECV. R^2 (values between 0 and 100%) shows the correlation of the NIR data with the reference values of the response parameter. The coefficient of determination R^2 should lie above 90 for quantitative calculation and above 70 for qualitative calculation. All models with values below 70 can not be used reasonably. Additionally, a precise model has a RMSECV as low as possible. A good and stable model should also not consist of many eigenvectors (referred to as "factors"), because the more factors are used the more unsteady the chemometric model becomes. So it is clear that the number of factors used should always stay in relation to the problem investigated. In the case of the investigation of nanocomposites the number of factors should preferably not be higher than 8.

RMSECV and R^2 are calculated the following:

$$\mathrm{RMSECV} = \sqrt{\frac{\sum_{i=1}^{n}(Y_{ki} - Y_{pi})^2}{n}}$$

$$R^2 = 1 - \frac{\sum_{i=1}^{n}(Y_{pi} - \overline{Y}_j)^2}{\sum_{i=1}^{n}(Y_{ki} - \overline{\overline{Y}}_j)^2}$$

Y_k. . .actual measurement value

Y_p. . .predicted value

$\overline{Y}, \overline{\overline{Y}}$. . . mean value

RESULTS AND DISCUSSION

Near infrared spectroscopy with Young's modulus as reference value

For this measurement, the response of interest is the Young's Modulus. The gained chemometric model should be close to the best model for the evaluation of the Young's Modulus values from NIR measurements. Very good correlation of tensile test and NIR measurements can be achieved by designing an optimized chemometric model. The chosen spectral pretreatment methods were mean centering and SNV. A coefficient of determination $R^2 = 97.70\%$ (factors = 5) with an RMSECV of 30 MPa for screw geometry 1 and $R^2 = 90.55\%$ (factors = 4) with an RMSECV of 94 MPa

TABLE I
Sample Description, Actual Values and Values Predicted by NIR for the Young's Modulus

Geometry	Clay/PP-MA content (wt %)	Screw speed (rpm)	Young's modulus (MPa)	NIR (MPa)
G1	5/5	100	2220	2230
		150	2190	2195
		200	2220	2214
		250	2200	2197
		300	2010	2074
G2	5/5	100	2340	2199
		150	2280	2275
		200	2260	2295
		250	2280	2237
		300	2210	2356

TABLE II
Sample Description, Actual Values, and Values Predicted by NIR for the Layer Distance

Geometry	Clay/PP-MA content (wt %)	Screw speed (rpm)	Layer distance (mN)	NIR (nm)
G1	5/5	100	42.35	2.708
		150	37.42	2.637
		200	31.56	2.599
		250	23.77	2.621
		300	17.23	2.716
G2	5/5	100	50.35	2.765
		150	45.32	2.677
		200	40.88	2.658
		250	36.53	2.602
		300	28.66	2.554

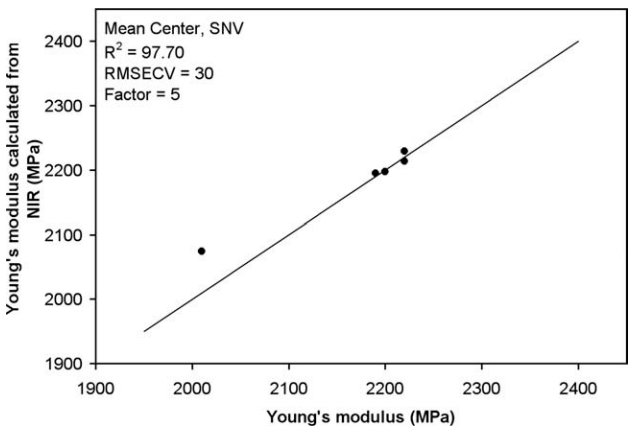

Figure 2 Young's modulus values calculated versus measured for geometry 1.

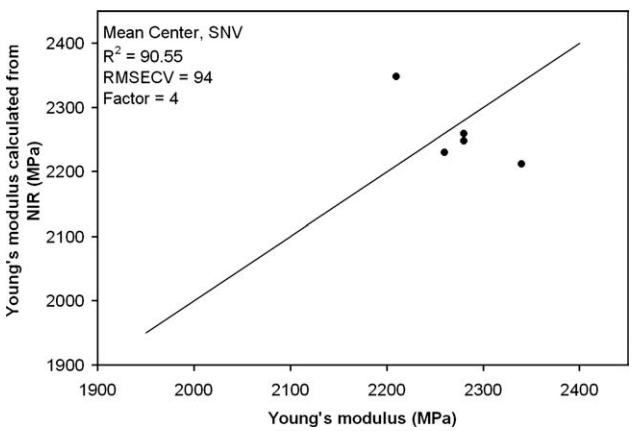

Figure 3 Young's modulus values calculated versus measured for geometry 2.

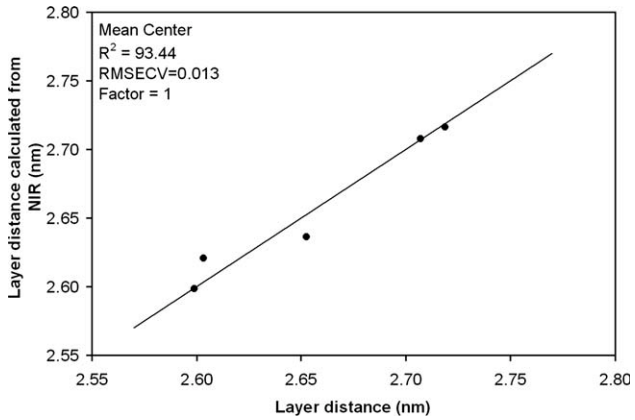

Figure 4 Layer distance calculated versus measured for geometry 1.

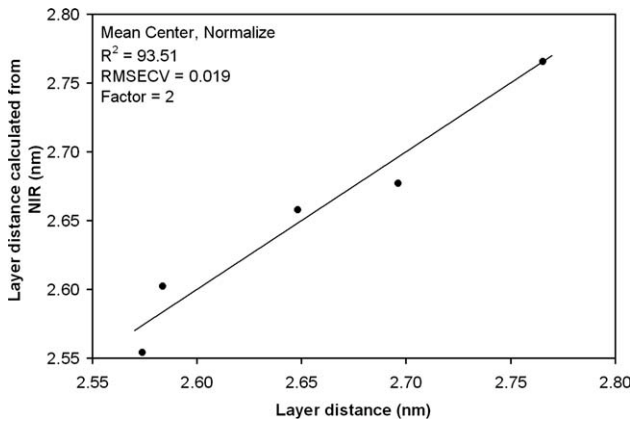

Figure 5 Layer distance calculated versus measured for geometry 2.

for screw geometry 2 could be achieved. Table I, Figures 2 and 3 show the results for both geometries.

The calculated Young's Moduli for geometry 1 are very close to the real values regarding that the performed tensile test has a mean standard deviation of 67 MPa.

The values for geometry 2 at screw speed 100 and 300 show greater deviations, which can be explained with the fact that cross validation is not always that efficient with extrapolation. Nevertheless, the values are quite precise regarding that the tensile test has a mean standard deviation of 166 MPa for geometry 2.

TABLE III
Sample Description, Actual Values, and Values Predicted by NIR for the Drawing Force

Geometry	Clay/PP-MA content (wt %)	Screw speed (rpm)	Drawing force (mN)	NIR (mN)
G1	5/5	100	42.35	40.30
		150	37.42	36.93
		200	31.56	29.39
		250	23.77	26.04
		300	17.23	12.83
G2	5/5	100	50.35	49.66
		150	45.32	43.39
		200	40.88	41.94
		250	36.53	37.68
		300	28.66	32.13

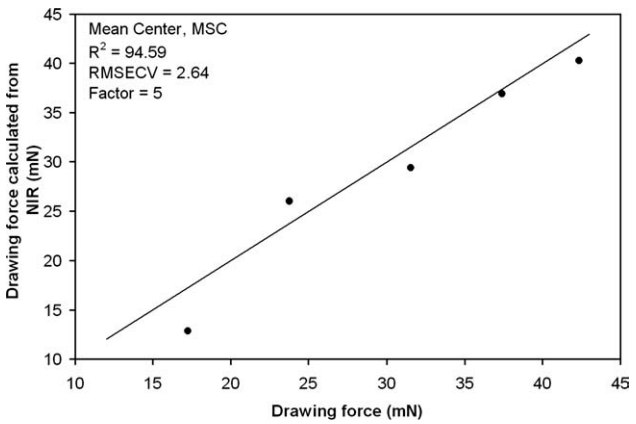

Figure 6 Drawing force calculated versus measured for geometry 1.

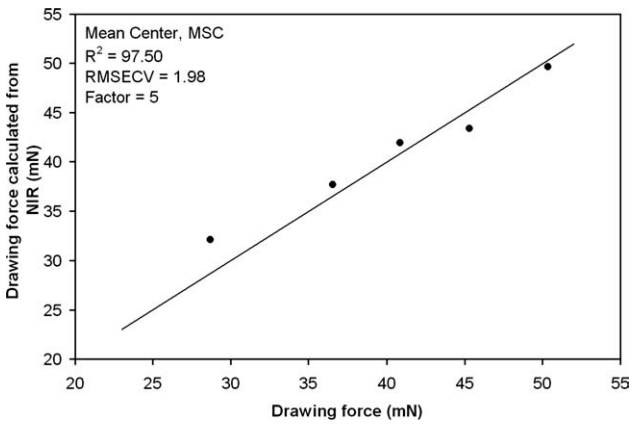

Figure 7 Drawing force calculated versus measured for geometry 2.

Near infrared spectroscopy with layer distance as reference value

The second response of interest is the interlayer distance gained by SAXS measurements. The interlayer distance is the spacing of one particle including the distance to the next particle. A very good correlation is achieved when the chemometric model is optimized with mean centering and normalization (Fig. 5). The coefficient of determination R^2 calculated for screw geometry 1 was 93.44% (factors = 1) with an RMSECV of 0.013 and R^2 = 93.51% (factors = 2) with an RMSECV of 0.019 nm for screw geometry 2. Table II, Figures 4 and 5 show the values for the layer distance calculated with the chemometrical model.

Near infrared spectroscopy with drawing force as reference value

The third response of interest is the on-line measured drawing force. To gain good correlation the chemometric model is optimized with mean centering and Multiplicative Scatter Correction (MSC). A coefficient of determination R^2 = 94.59% (factors = 5) with an RMSECV of 2.64 mN for screw geometry 1 and R^2 = 97.50% (factors = 5) with an RMSECV of 1.98 mN for screw geometry 2 could be achieved. Table III, Figures 6 and 7 show the results measured and calculated for both geometries.

CONCLUSIONS

As shown in this work the Young's Modulus, the layer distance and the drawing force exhibit good correlation with NIR data analyzed by PLS 1 algorithm. It can bee seen that near infrared spectroscopy is a quantitative method for monitoring nanocomposite quality although the measurements were done at different aggregate states and samples with different processing history caused by sample preparation. Therefore important parameters like crystallization could not be considered by the NIR measurements. It is evident that the different aggregate states (melt state vs. semicrystalline solid state) and the postprocessing procedures (cooling down, heating up, molding, and cooling down again) causing for example preferential orientations, are affecting the chemometric models negatively. Nevertheless this work shows that it is possible to determine the Young's modulus, the layer distance and the drawing force with sufficient precision for quantitative evaluation with near infrared spectroscopy. Therefore NIR spectroscopy is perfectly suitable for inline quality control and characterization of nanocomposites in real time and directly in the melt during production, leading to a faster composite optimization process with reduced rejections and costs.

Parts of the FTNIR research work were done within the FH Plus - Project AMiESP (Advanced Methods in Embedded Signal Processing).

References

1. Vaia, R. A.; Jandt, K. D.; Kramer, E. J.; Giannelis, E. P. Chem Mater 1996, 8, 2628.
2. Davis, C. H.; Mathias, L. J.; Gilman, J. W.; Schiraldi, D. A.; Shields, J. R.; Trulove, P.; Sutto, T. E.; Delong, H. C. J Polym Sci Part B: Polym Phys 2002, 40, 2661.
3. Pinnavaia, T. J.; Beall, G. W. Polymer-Clay Nanocomposites; John Wiley & Sons: New York, 2000.
4. Laske, S.; Kracalik, M.; Feuchter, M.; Pinter, G.; Maier, G.; Märzinger, W.; Haberkorn, M.; Langecker, G. R. J Appl Polym Sci 2009, 114, 2488.
5. Heigl, N.; Petter, C. H.; Rainer, M.; Najam-Ul-Haq, M.; Vallant, R.; Bakry, R.; Bonn, G.; Huck, C. J Near Infrared Spectrosc 2007, 15, 269.
6. D. Fischer, I. Alig, J. Hutschenreuter, Presented at the 21st Annual Meeting of the Polymer Processing Society (PPS21), Leipzig, 2005.
7. Fischer, D.; Kirschner, U. GIT 2002, 11, 1267.
8. Barnes, S.; Sibley, M.; Brown, E.; Edwards, H.; Scowen, I.; Coates, P. Annu Tech Conference 2003, 3, 3311.
9. Fischer, D.; Sahre, K.; Abdelrhim, M.; Voit, B.; Sadhu, V.; Pionteck, J.; Komber, H.; Hutschenreuter, J. CR Chimie 2006, 9, 1419.
10. Barrès, C.; Bounor-Legaré, V.; Melis, F.; Michel, A. Polym Eng Sci 2006, 46, 1613.
11. Watari, M.; Ozaki, Y. Appl Spectrosc 2006, 60, 529.
12. Nagata, T.; Ohshima, M.; Tanigaki, M. Polym Eng Sci 2000, 40, 1107.
13. Barnes, S.; Brown, E.; Sibley, M.; Edwards, H.; Scowen, I.; Coates, P. Appl Spectrosc 2005, 59, 611.
14. Barnes, S.; Brown, E.; Sibley, M.; Edwards, H.; Coates, P. Analyst 2005, 130, 286.
15. Steinhoff, B.; Lellinger, D.; Pötschke, P.; Alig, I. Presented at the 21st Annual Meeting of the Polymer Processing Society (PPS21), Leipzig, 2005.
16. Asai, K.; Okamoto, M.; Tashiro, K. Polymer 2008, 49, 5186.
17. Bokobza, L.; Diop, A.; Fournier, V.; Minne, J.; Brunell, J. Macromol Symp 2005, 230, 87.
18. Higgins, J.; Arrivo, S.; Thurau, G.; Green, R.; Bowen, W.; Lange, A.; Templeton, A.; Thomas, D.; Reed, R. Anal Chem 2003, 75, 1777.
19. Balta-Calleja, F. J.; Vonk, C. G. X-Ray Scattering of Synthetic Polymers; Elsevier: New York, 1989.
20. Strobl, G. R.; Schneider, M. J Polym Sci 1980, 18, 1343.
21. Laske, S.; Kracalik, M.; Gschweitl, M.; Feuchter, M.; Maier, G.; Pinter, G.; Thomann, R.; Friesenbichler, W.; Langecker, G. R. J Appl Polym Sci 2009, 111, 2253.